

Interplay between charge, orbital and magnetic order in $\text{Pr}_{1-x}\text{Ca}_x\text{MnO}_3$

M. v. Zimmermann¹, J.P. Hill¹, Doon Gibbs¹, M. Blume¹, D. Casa², B. Keimer^{2,3}, Y. Murakami⁴, Y. Tomioka⁵, and Y. Tokura⁶

¹*Department of Physics, Brookhaven National Laboratory, Upton, New York 11973, USA*

²*Department of Physics, Princeton University, New Jersey 08544, USA*

³*Max-Planck-Institut für Festkörperforschung, 70569, Stuttgart, Germany.*

⁴*Photon Factory, Institute of Materials Structure Science, High Energy Accelerator Research Organization, Tsukuba, 305-0801, Japan*

⁵*Joint Research Center for Atom Technology (JRCAT), Tsukuba 305-0046, Japan*

⁶*Department of Applied Physics, University of Tokyo, Tokyo 113-0033, Japan and JRCAT*

We report resonant x-ray scattering studies of charge and orbital order in $\text{Pr}_{1-x}\text{Ca}_x\text{MnO}_3$ with $x=0.4$ and 0.5. Below the ordering temperature, $T_O=245$ K, the charge and orbital order intensities follow the same temperature dependence, including an increase at the antiferromagnetic ordering temperature, T_N . High resolution measurements reveal, however, that long range orbital order is never achieved. Rather, an orbital domain state is formed. Above T_O , the charge order fluctuations are more highly correlated than the orbital fluctuations. Similar phenomenology is observed in a magnetic field. We conclude that the charge order drives the orbital order at the transition.

Disentangling the origins of high temperature superconductivity and colossal magnetoresistance in the transition metal oxides remains at the center of current activity in condensed matter physics. An important aspect of these strongly correlated systems is that no single degree of freedom dominates their response. Rather, the ground state properties are thought to reflect a balance among several correlated processes, including orbital and charge order, magnetism, and coupling to the lattice.

The perovskite manganites provide an especially illuminating example of the interplay among these interactions, since in these materials the balance may be altered by doping, among other things. As a result, much work has been done to understand their magnetic ground states and lattice distortions, dating back to the seminal experiments of Wollan and Koehler [1]. Less is known about the roles of charge and orbital order, for which (until recently) there has been no direct experimental probe. The classic work of Goodenough [2] has nevertheless served as a guide to their ordered arrangements, as supplemented by measurements of the temperature dependence of the lattice constants, and other properties. Recently this situation has changed with the detection of charge and orbital order by x-ray resonant scattering techniques. [3–10]. Specifically, it has been found that the sensitivity of x-ray scattering to these structures is dramatically enhanced by tuning the incident x-ray energy to the Mn K-absorption edge. Thus, it is now possible to characterize the orbital and charge order distributions directly, and to study their response to changes of temperature or magnetic field.

In this paper, we report x-ray resonant scattering studies of $\text{Pr}_{1-x}\text{Ca}_x\text{MnO}_3$ with $x=0.4$ and 0.5 . We have detected both charge and orbital order below a common phase transition temperature ($T_O=245$ K), and confirmed the ground state originally proposed by Goodenough for the isostructural compound $\text{La}_{0.5}\text{Ca}_{0.5}\text{MnO}_3$ [2]. Below the transition, we find that the intensities of the charge and orbital order have the same temperature dependences, suggesting that they are linearly coupled. There is, moreover, a notable increase of the scattering at the Néel temperature ($T_N=170$ K), implying a coupling of the orbital and magnetic degrees of freedom. Intriguingly, high momentum transfer resolution measurements reveal that long range orbital order is never achieved at these concentrations. Rather, a domain state is formed at low temperature. At temperatures above T_O , we observe critical charge and orbital scattering. Remarkably, the correlation lengths differ, with the length scale of the charge order exceeding that of the orbital order. From this we conclude that charge order drives the orbital order in these systems. This picture is supported by studies in which the phase transition is driven by an applied magnetic field.

For small x , $\text{Pr}_{1-x}\text{Ca}_x\text{MnO}_3$ has an orbitally ordered ground state at low temperature analogous to that ob-

served in LaMnO_3 . The electronic configuration of the Mn^{3+} ions is (t_{2g}^3, e_g^1) , with the t_{2g} electrons localized. The e_g orbitals are hybridized with the oxygen p orbitals, and participate in a cooperative Jahn-Teller distortion of the MnO_6 octahedra. This leads to $(3x^2 - r^2) - (3y^2 - r^2)$ -type orbital order of the e_g electrons in the ab -plane. For $0.3 \leq x \leq 0.7$, charge order among Mn^{3+} and Mn^{4+} ions is believed to occur in addition to the orbital order. The fraction of Mn ions in the Mn^{4+} state equals the concentration of Ca ions. Thus, by varying the Ca concentration, it is possible to alter the balance between the charge and orbital order. The proposed ground state for $x=0.4$, including charge, orbital and magnetic order, is illustrated in fig. 1b [2,11,12]. In orthorhombic notation, for which the fundamental Bragg peaks occur at $(0,2k,0)$ with k integer, the charge order reflections occur at $(0,2k+1,0)$ and the orbital order reflections at $(0, k+\frac{1}{2},0)$. The magnetic structure is of the modified CE-type [11].

The single crystals used in this study were grown by a float zone technique. $(0,1,0)$ surfaces were cut and polished giving mosaic spreads of $\sim 0.25^\circ$. X-ray scattering experiments were carried out at the National Synchrotron Light Source on Beamlines X22B and C. X22C utilizes a vertical scattering geometry with an incident energy resolution of ~ 5 eV. Two analyzer configurations were used. The first, a $\text{Ge}(111)$ crystal, provided an effective resolution of $7.2 \times 10^{-4} \text{ \AA}^{-1}$ (HWHM) at the $(0,2,0)$ reflection. The second provided linear polarization analysis of the scattered beam with a Cu (220) crystal [13]. The incident polarization was 95% linearly polarized in the horizontal plane (σ). Experiments in a magnetic field were performed on X22B in a horizontal scattering geometry.

The present experiments were carried out using x-ray resonance scattering techniques. As shown in a series of recent papers [3–10], scattering from orbital and charge order in transition metal oxides is enhanced when the incident x-ray energy is tuned near the K absorption edge. In the dipole approximation, this corresponds to a $1s \rightarrow 4p$ transition of a virtually excited electron at the metal site. The sensitivity to orbital order in manganites arises from the splitting of the Mn 4p levels by the 3d levels, which is mainly associated with the Jahn-Teller distortion [7,10]. The sensitivity to charge order originates in the small difference in K-absorption energies associated with the Mn^{3+} and Mn^{4+} sites, leading to anomalous scattering at the difference reflections [3].

The inset of fig. 1 shows the energy dependence of the intensities of the charge and orbital order as the incident photon energy is tuned through the K absorption edge. The data were taken at the $(0,3,0)$ and $(0,2,5,0)$ reflections, respectively, of the $x=0.4$ sample. Each scan shows an enhancement at 6.555 keV, characteristic of dipole resonant scattering. Maximum count rates of about 800 and 3000 s^{-1} were obtained for the orbital

and charge order scattering, respectively, with a Ge(111) analyzer. The structure observed in the lineshape for the charge order reflects the interference of the resonant and nonresonant contributions, and will be discussed in detail elsewhere [14]. In addition to the resonance, both the charge and orbital order intensities exhibited a $\sin^2(\psi)$ dependence on the azimuthal angle, ψ , at resonance [3,4]. This angle defines rotations of the sample about the scattering vector. Polarization analysis further revealed that the orbital scattering is predominantly rotated (σ - π), whereas the charge scattering is mainly unrotated (σ - σ). These results are consistent with predictions of the resonant cross-section for orbital and charge order [3–5], and confirm the original picture of charge and orbital order given for this class of compounds by Goodenough [2] (fig. 1b).

The temperature dependences of the charge and orbital order obtained at resonance for the $x=0.4$ sample are shown in fig. 1. For comparison purposes the intensities have been scaled together at 10 K. Between 10 and 120 K, both intensities are approximately constant, but decrease by about 25% on passing through the Néel temperature ($T_N=170$ K). They drop sharply to zero at $T_O=245$ K. This is coincident with an orthorhombic-to-orthorhombic structural transition, as determined from high-resolution measurements of the lattice constants [14]. It follows that the temperature dependences of the charge and orbital order are identical, which suggests that the corresponding order parameters are linearly coupled. It seems clear in this regard that the growth of orbital (and charge) order below 245 K enhances the antiferromagnetic correlations, and thereby promotes the magnetic phase transition. This is consistent with the results of inelastic neutron scattering studies of (Bi,Ca)MnO₃, in which orbital order was found to quench ferromagnetic fluctuations [15]. Qualitatively similar results have been found for the $x=0.5$ sample [14].

The behavior of the charge and orbital scattering in the vicinity of the structural phase transition at T_O is illustrated for the $x=0.4$ sample in fig. 2. Longitudinal scans were taken (upon warming) of the (0,3,0) reflection in a σ - σ geometry and of the (0,2.5,0) reflection in a σ - π geometry. We find that a measurable intensity of the charge order fluctuations (shown on a log scale in fig. 2a) persists to much higher temperatures above T_O than the orbital order fluctuations. The corresponding peak widths are considerably narrower for the charge order (fig. 2b), implying that the correlation lengths of the charge order are longer than those of the orbital order at any given temperature above T_O [16].

The picture these data then present is one in which the phase transition proceeds via local charge order fluctuations which grow as the transition is approached, nucleating long range order at the transition temperature. The orbital fluctuations are induced by these charge fluctuations through the coupling discussed above, and become

observable only close to the transition.

The phase transition may also be driven by applying a magnetic field, as demonstrated by Tomioka *et al.* [17]. It is an interesting question whether the same phenomenology of the fluctuations applies when the temperature is held fixed. We have carried out studies of the transition at two temperatures, T=30 K and 200 K, with critical fields of $H_O=6.9(1)$ T, and $H_O=10.4$ T, respectively. Data taken at T=30 K are illustrated in fig. 3. The two order parameters exhibit identical field dependences below the transition. Above the transition, the charge order fluctuations are markedly stronger than the orbital fluctuations. Similar behavior was observed at T=200 K, i.e. charge order fluctuations were observed at fields for which orbital fluctuations were no longer observable (inset fig. 3). Thus, it appears that the transition is driven by charge order fluctuations for both temperature and field driven cases. (As a result of experimental constraints, it was only possible to measure charge and orbital order scattering at a photon energy of 8 keV in an applied magnetic field. The corresponding nonresonant intensities are sufficiently weak above T_O that it was not possible to obtain reliable values of the half-width).

Finally, we performed high q-resolution measurements of the charge and orbital order below T_O to investigate the extent of their order in detail. Remarkably, in the $x=0.4$ sample, we found an orbital order correlation length of $\xi_{OO}=320\pm10$ Å and a charge order correlation length of $\xi_{CO}\geq2000$ Å. This difference is even more apparent in the $x=0.5$ sample, as shown in fig. 4. Here longitudinal scans through the (0,2,0), (0,1,0) and (0,2.5,0) reflections are superimposed for comparison. The width of the (0,2,0) scan approximates the effective resolution. The (0,1,0) charge order reflection shows only a slight broadening ($9.1(1)\cdot10^{-4}$ Å⁻¹), corresponding to a correlation length of $\xi_{CO}\geq2000$ Å [18]. The orbital order, however, is substantially broadened, with a correlation length of $\xi_{OO}=160\pm10$ Å [19]. It follows that the orbitals do not exhibit long range order, but instead form a domain state with randomly distributed anti-phase domain walls (see fig. 1b). In contrast, the charge order is much more highly correlated.

A possible explanation for the difference in orbital domain sizes observed in the two samples follows from the fact that the $x=0.5$ sample is closer to tetragonal than the $x=0.4$ sample: $\delta(x=0.5)=\frac{2(a-b)}{(a+b)}=1.48\times10^{-3}$ compared to $\delta(x=0.4)=4.23\times10^{-3}$ at room temperature [11]. In the more tetragonal sample the a and b domains are nearly degenerate and the energetic cost of an orbital domain wall is correspondingly reduced [20].

The presence of an orbital domain state is consistent with powder neutron diffraction studies of La_{0.5}Ca_{0.5}MnO₃, which also exhibits the CE magnetic structure with orbital and charge order [21]. In this material, magnetic correlation lengths of $\xi_{3+}=200-400$

\AA and $\xi_{4+} \geq 2000 \text{\AA}$ were found for the respective sub-lattices, and anti-phase domain walls were postulated to explain the disorder. It seems likely that these domain walls are in fact the orbital domain walls observed in the present experiment, which lead to magnetic disorder through the coupling mentioned above. The presence of such orbital domain boundaries breaks the magnetic coherence of the 3+ sublattice only, as long as charge order is preserved (fig. 1b). These results taken together suggest that orbital domain states may be common to these systems – at least in this range of doping.

In summary, we have used resonant x-ray scattering techniques to study the development of charge and orbital order in doped manganites, $\text{Pr}_{1-x}\text{Ca}_x\text{MnO}_3$, with $x=0.4$ and 0.5. We have found that the transition into a charge and orbitally ordered state proceeds via charge order fluctuations, which grow as the transition is approached from above, until at an abrupt, first-order-like, transition long range charge order is nucleated. At the same time, less well correlated orbital fluctuations are observed. While the correlation length of the orbital order grows as the transition is approached, long range order is not achieved, and below the charge order transition an orbital domain state is observed. The orbital correlation length appears to be concentration dependent, with a more highly correlated orbital state being observed in the $x=0.4$ sample. Phenomenologically similar behavior is observed when the phase transition is driven by a magnetic field. Below the transition, the charge and orbital order parameters exhibit identical temperature dependences, indicative of a linear coupling between these degrees of freedom. At the Néel temperature a jump in their intensities is observed demonstrating the importance of the magnetic -charge/orbital order coupling in these systems.

We acknowledge useful conversations with A.J. Millis and G.A. Sawatzky. The work at Brookhaven was supported by the U.S. Department of Energy, Division of Materials Science, under Contract No. DE-AC02-98CH10886 and at Princeton University by the N.S.F., under grant DMR-9701991. Support from the Ministry of Education, Science and Culture, Japan, by the New Energy and Industrial Technology Development Organization (NEDO) and by the Core Research for Evolutional Science and Technology (CREST) is also acknowledged.

- [5] S. Ishihara and S. Maekawa, Phys. Rev. Lett. **80** 3799, (1998).
- [6] M. Fabrizio, M. Altarelli and M. Benfatto, Phys. Rev. Lett., **80** 3400 (1998), *ibid* **81** 4030 (1998).
- [7] I.S. Elfimov, V.I. Anisimov and G.A. Sawatzky cond-mat/9901058.
- [8] Y. Endoh *et al.*, cond-mat/9901148.
- [9] L. Paolasini *et al.*, preprint.
- [10] M. Benfatto, Y. Joly and C. R. Natoli, preprint.
- [11] Z. Jirák *et al.*, J. of Mag. and Mag. Mat. **53**, 153, (1985).
- [12] Y. Okimoto *et al.*, Phys. Rev. B **57**, R9377 (1998).
- [13] D. Gibbs *et al.*, Rev. Sci. Instrum., **60** 1655 (1988).
- [14] M. v. Zimmermann *et al.*, in preparation.
- [15] Wei Bao *et al.*, Phys. Rev. Lett. **78** 543, (1997).
- [16] The correlation length of the charge order must be at least as long as that of the orbital order, since the unit cell of the orbital order is defined on the charge order lattice.
- [17] Y. Tomioka *et al.*, Phys. Rev. B **53**, R1689 (1996).
- [18] As estimated by performing a 1-d deconvolution of the resolution and using $\xi = \frac{b}{2\pi\Delta k}$, were Δk is the fitted HWHM.
- [19] Note that although the resolution function exhibits some q -dependence, the observed broadening is much too large to be explained by such effects.
- [20] A.J. Millis, private communication.
- [21] P.G. Radaelli *et al.*, Phys. Rev. B **55** (1997) 3015.

FIG. 1. a: Orbital and charge order parameters versus temperature for the $x = .4$ sample. Open and closed circles: Resonant intensities of the orbital and charge order measured at the $(0,1.5,0)$ and $(0,3,0)$ reflections, respectively. Inset: Energy dependence of the orbital and charge order peaks in the $\sigma\text{-}\pi$ and $\sigma\text{-}\sigma$ geometries, respectively. b: schematic of charge and orbital order, showing an orbital anti phase domain boundary (dashed line) in the ab -plane. Black points represent Mn^{4+} and open symbols Mn^{3+} . The arrows indicate the magnetic ordering. The dotted and solid lines show the charge and orbital unit cells, respectively.

FIG. 2. a) Temperature dependence of the peak intensities of the charge (closed circles) and orbital (open circles) for the $x = 0.4$ sample. b) Temperature dependence of the half widths at half maximum (HWHM).

FIG. 3. Charge and orbital order as function of magnetic field at 30 K. The intensities of the two peaks have been scaled to agree at low fields. Inset: Charge and orbital order superlattice reflection at 198 K and 11 T. The orbital order is no longer observable, but scattering from charge order remains clearly visible.

FIG. 4. a: Longitudinal scans of the $(0\ 2\ 0)$ Bragg reflection, the $(0\ 1\ 0)$ charge order peak and the $(0\ 2.5\ 0)$ orbital order peak.

- [1] E.O. Wollan and W.C. Koehler, Phys. Rev. **100**, 545, (1955).
- [2] J.B. Goodenough, Phys. Rev. **100**, 555, (1955).
- [3] Y. Murakami *et al.*, Phys. Rev. Lett. **80**, 1932, (1998).
- [4] Y. Murakami *et al.*, Phys. Rev. Lett. **81**, 582, (1998).

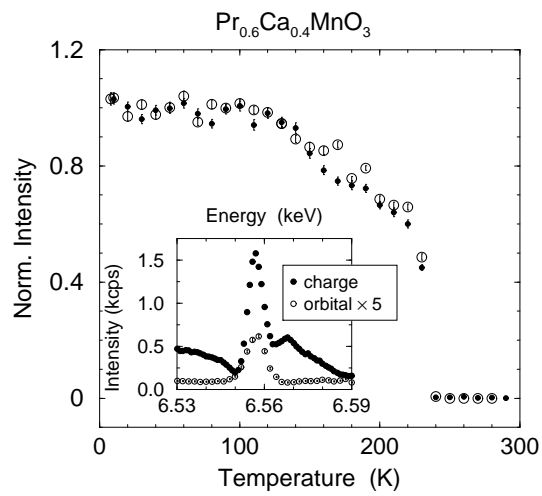


fig. 1a v. Zimmermann *et al.*

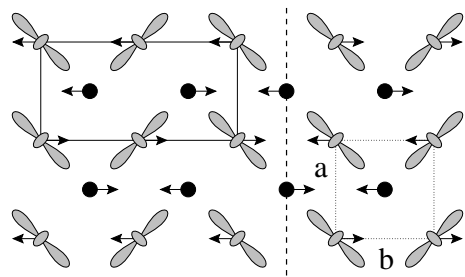


fig. 1b

v. Zimmermann *et al.*

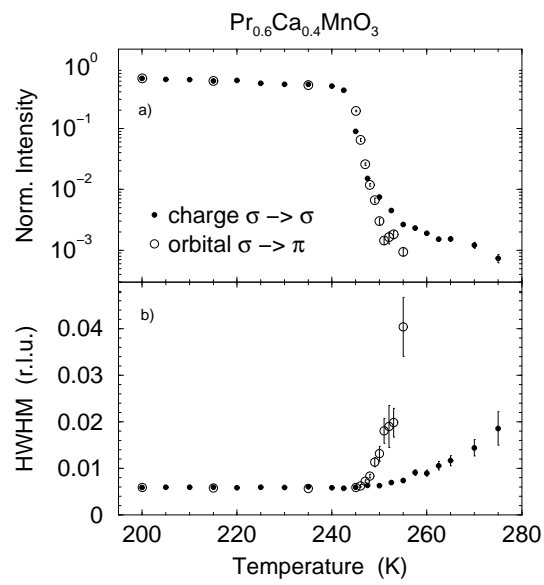


fig. 2

v. Zimmermann *et al.*

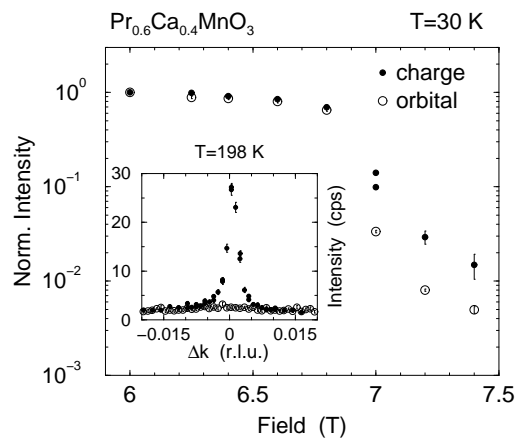


fig. 3

v. Zimmermann *et al.*

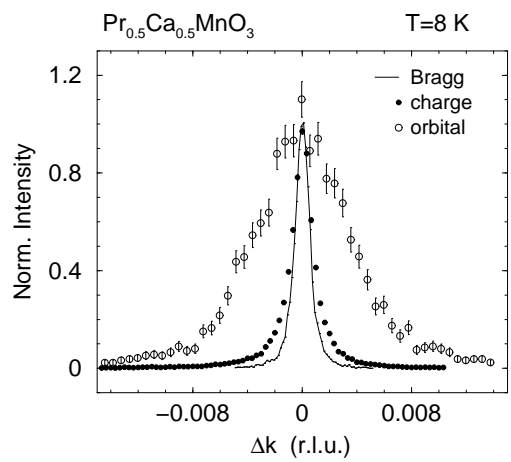


fig.4

v. Zimmermann *et al.*